Supporting Information

Unlocking High-Performance Lithium Metal Batteries through a Unique Solvation Structure Engineered by an Ether Solvent

Thanh Cham Le[a], Thuy Duong Pham[b]*, and Kyung-Koo Lee[a]*

[a] *Department of Chemistry, Kunsan National University, Gunsan, Jeonbuk, 54150, Republic of Korea*

[b] *Faculty of Biotechnology Chemistry and Environmental Engineering, Phenikaa School of Engineering, Phenikaa University, Hanoi 10000, Vietnam*

E-mail address: duong.phamthuy@phenikaa-uni.edu.vn (T. D. Pham) and kklee@kunsan.ac.kr (K.-K. Lee)

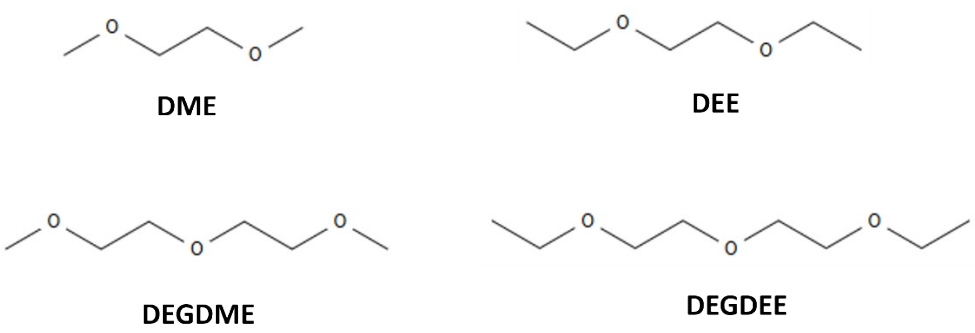

Fig. S1. Molecular structure of different ether solvents.

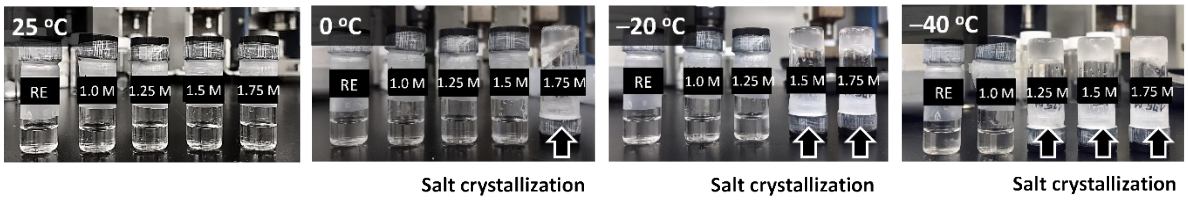

Fig. S2. The state of the 1.0 M $LiPF_6$-EC: EMC:DMC (1:1:1, vol.) (denoted as RE) and LiFSI in DEGDEE electrolytes with different concentrations at various temperatures.

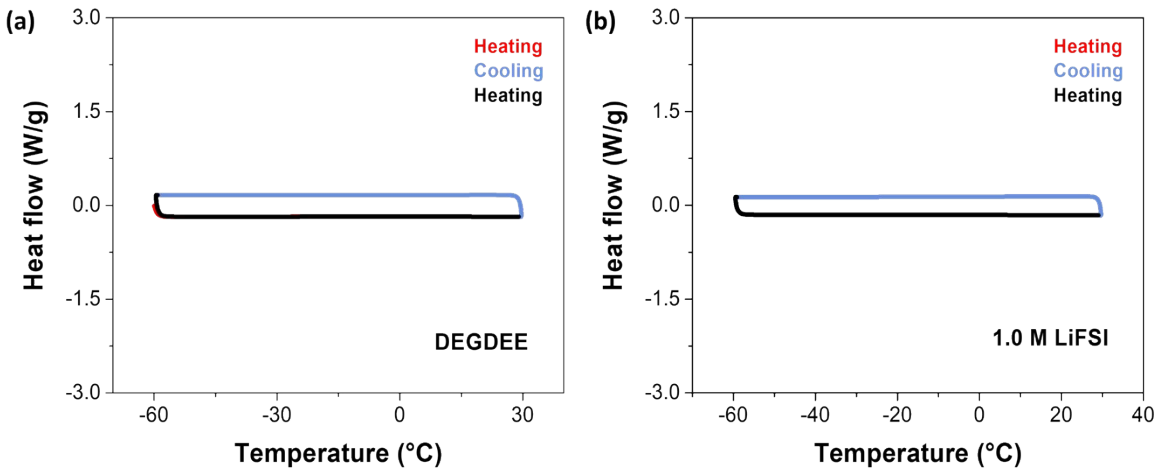

Fig. S3. DSC of (a) pure DEGDEE solvent and (b) 1.0 M LiFSI-DEGDEE.

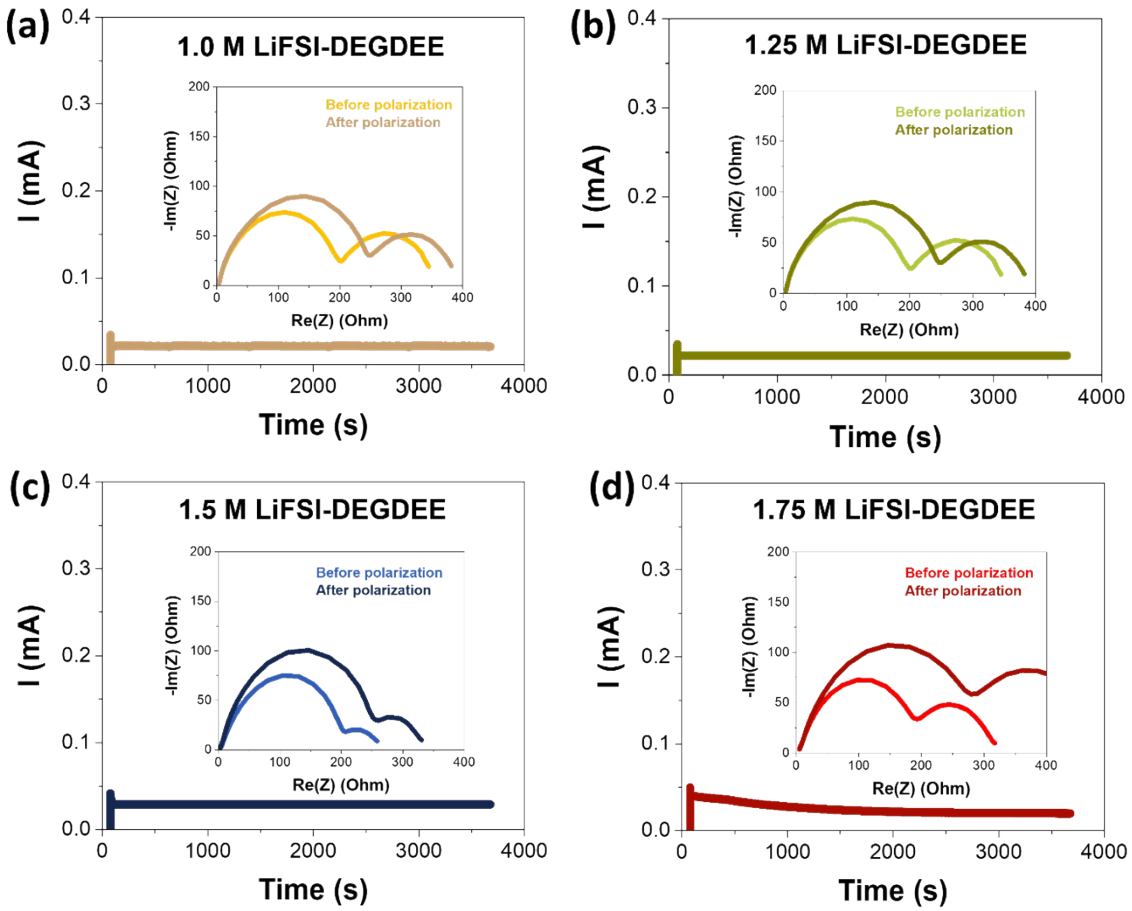

Fig. S4. Transference number of Li (t_+) in the investigated electrolyte.

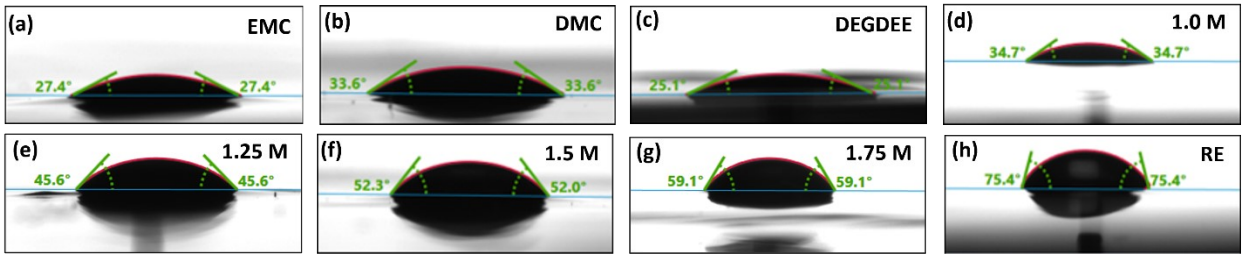

Fig. S5. Contact angle images of (a–c) pure solvents and (d–h) DEGEEE-based electrolytes at different concentrations on PP separators at room temperature.

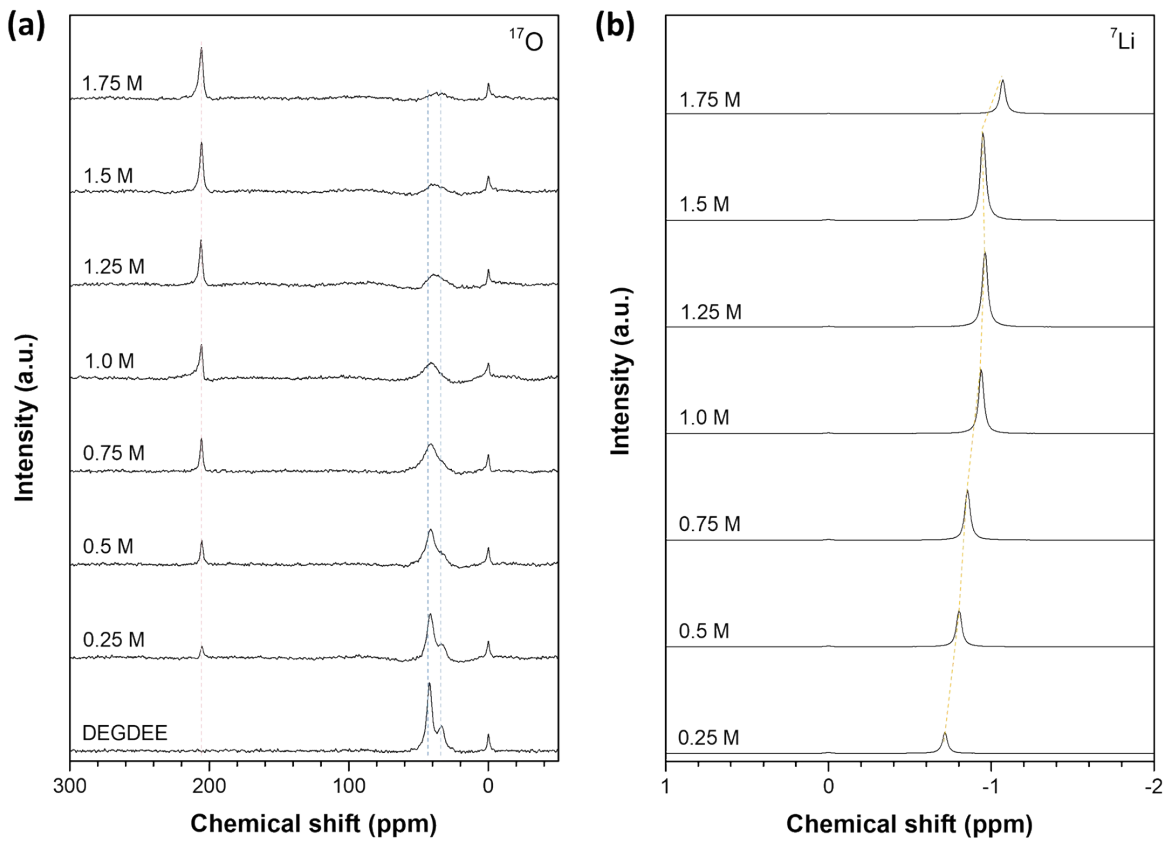

Fig. S6. NMR spectra of LiFSI/DEGDEE electrolytes at different concentrations. (a) ^{17}O-NMR spectra and (b) ^{7}Li-NMR spectra.

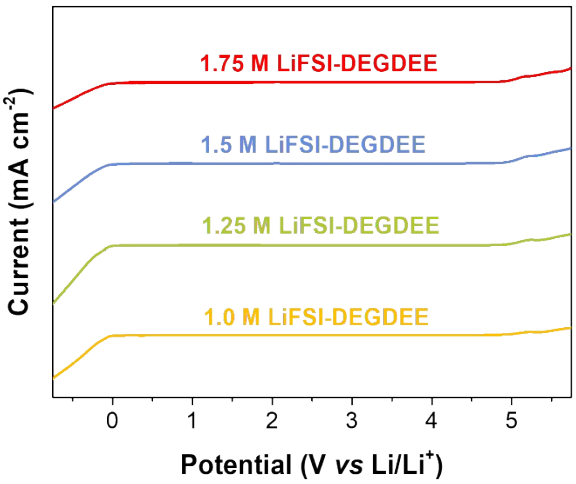

Fig. S7. LSV of different concentrations of LiFSI in DEGDEE on Pt electrodes in a three-electrode cell with a scan rate of 2 mV s^{-1}.

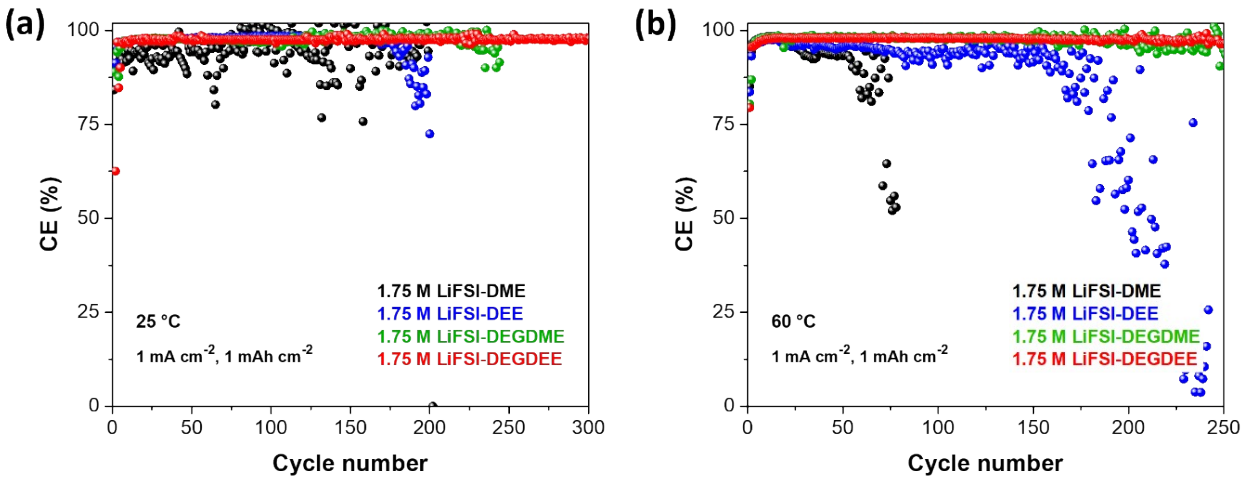

Fig. S8. Comparison of CE for Li plating/stripping in Li||Cu cells cycling with 1.75 M LiFSI in various linear ether solvents at (a) 25 °C and (b) 60 °C.

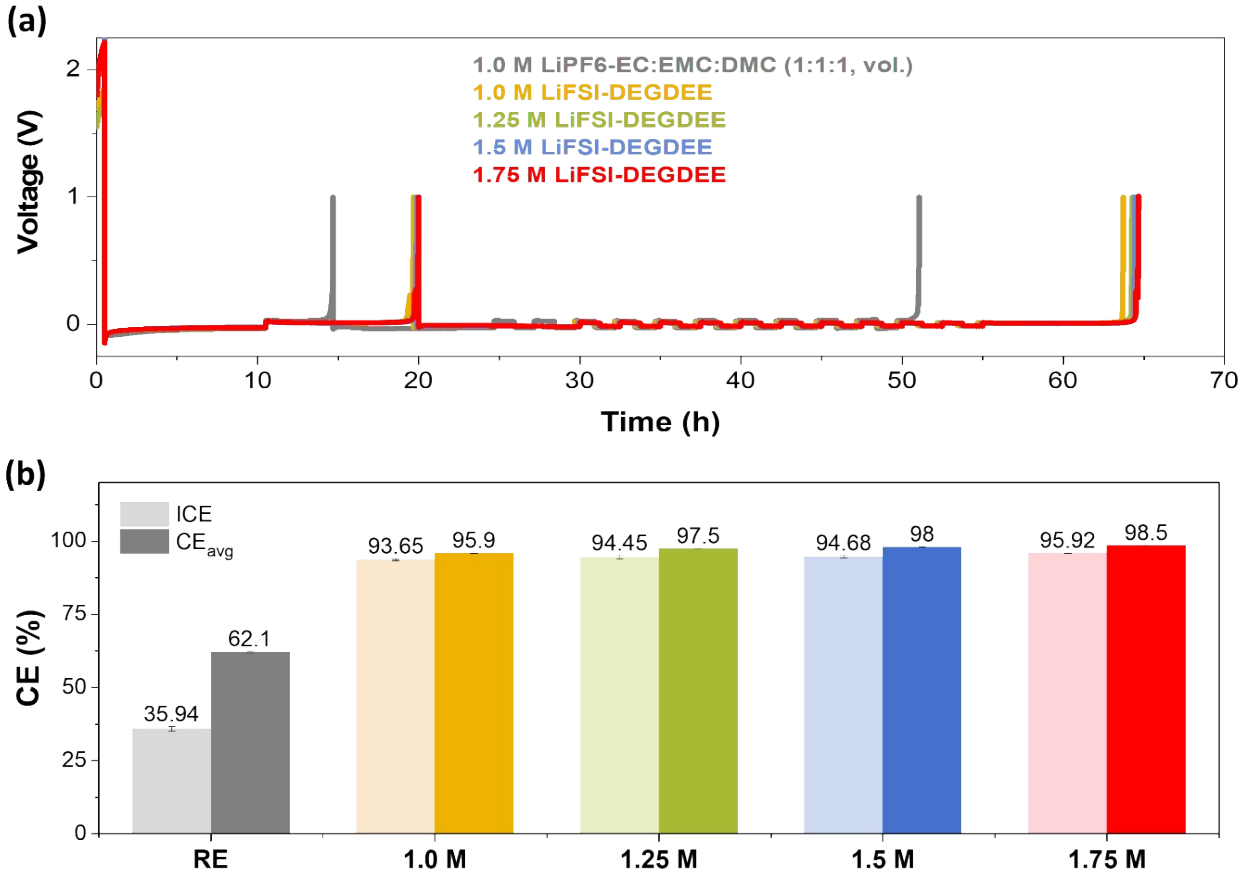

Fig. S9. Aurbach measurement of Li metal CEs in asymmetric half cells with Cu electrode of RE (1.0 M $LiPF_6$-EC:EMC:DMC (1:1:1, v/v)) and different concentrations of LiFSI–DEGDEE electrolytes. (a) Voltage profiles of Li||Cu cells. (b) Initial CE (ICE) and Average CE (CE_{avg}).

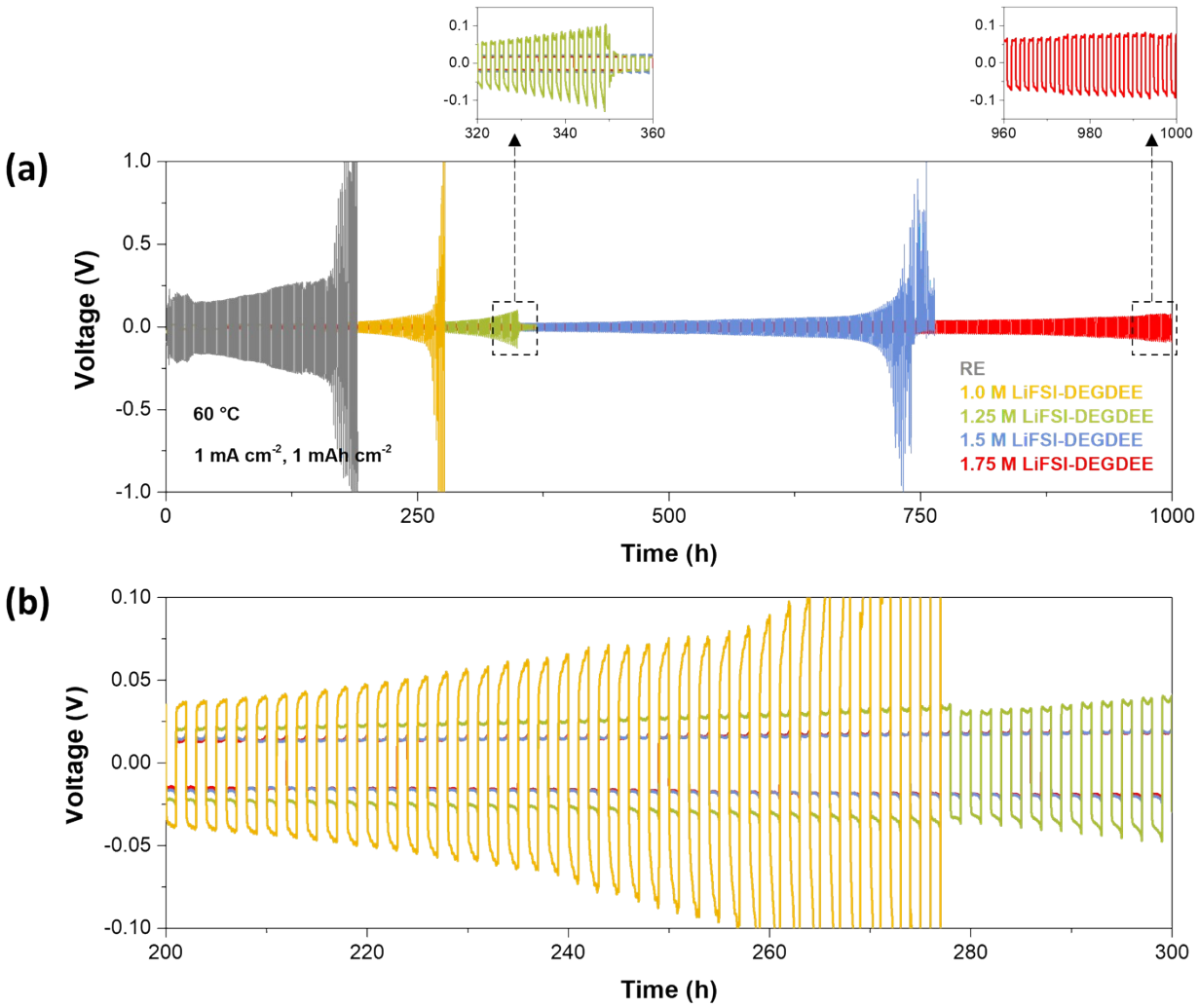

Fig. S10. (a) Voltage profiles of Li||Li symmetric cells cycling in the electrolytes at 60 °C and (b) an enlarged region.

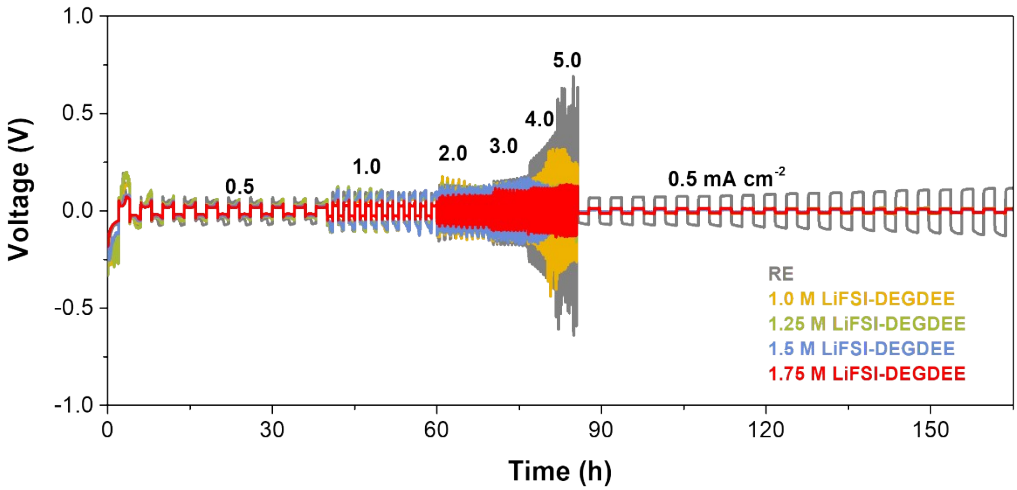

Fig. S11. Rate capability performance of Li||Li cells at low to moderate current densities and capacity of 1.0 mAh cm^{-2} in the different electrolytes.

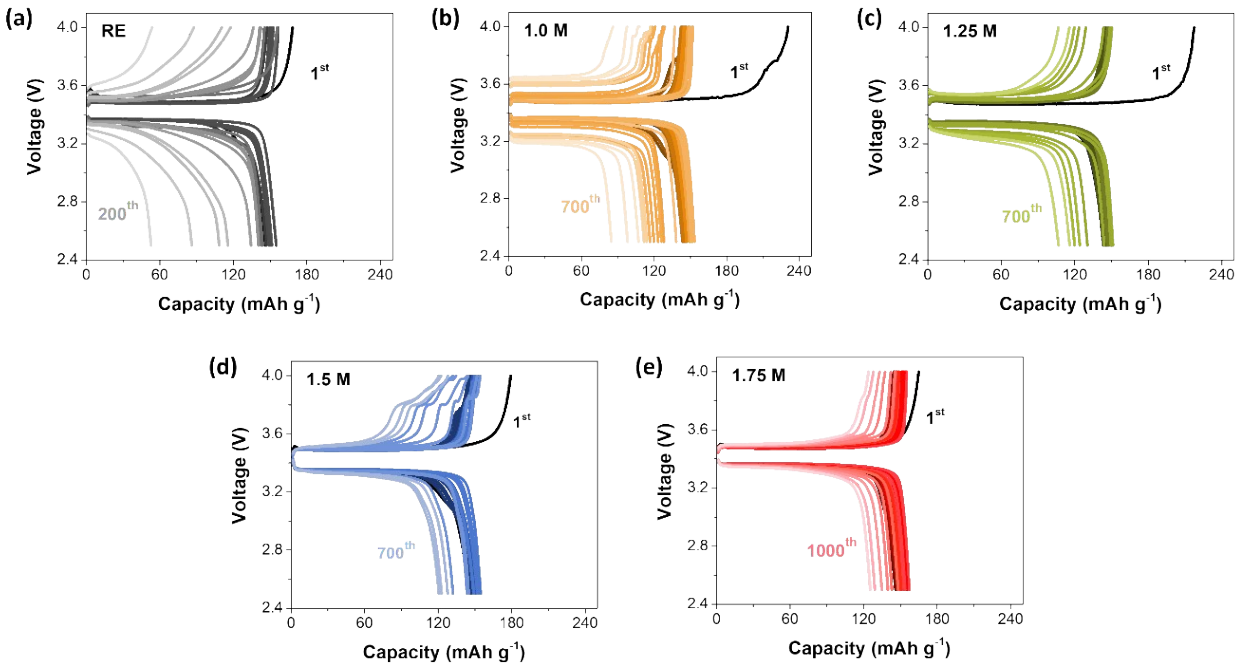

Fig. S12. Voltage profile of Li||LFP full cells cycled in (a) RE, (b-e) various LiFSI-DEGDEE electrolytes at charge/discharge current density of 1.0 C/1.0 C at 25 °C.

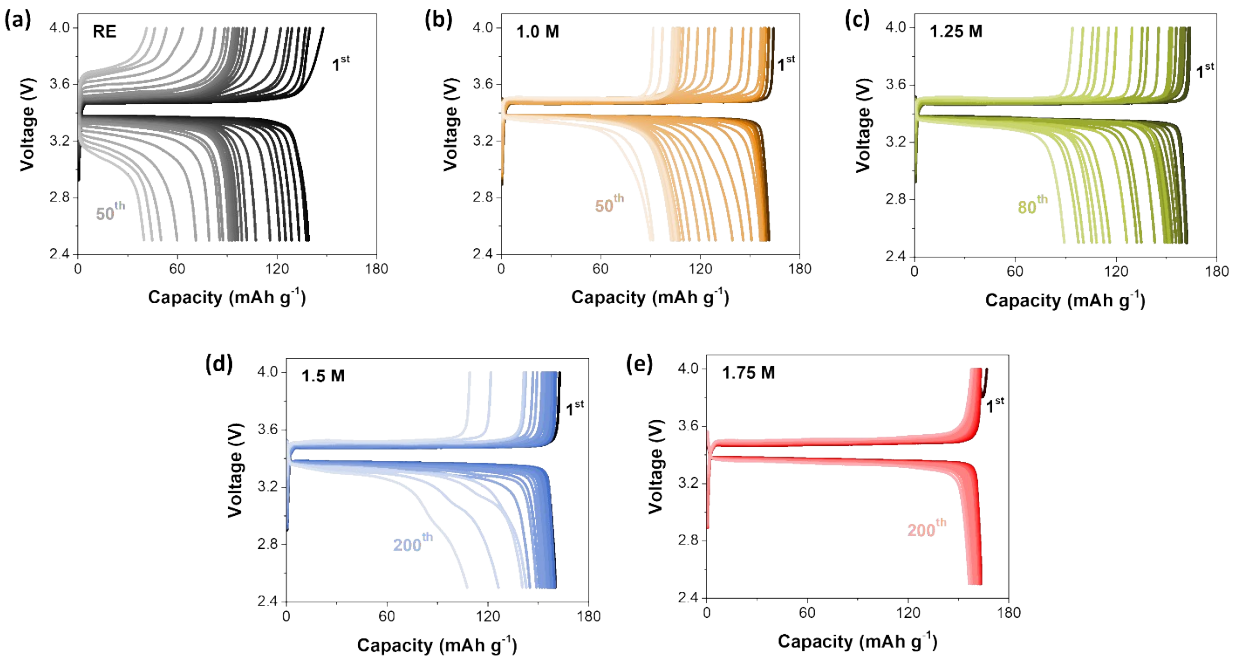

Fig. S13. Voltage profile of Li||LFP full cells cycled in (a) RE, (b-e) various LiFSI-DEGDEE electrolytes at charge/discharge current density of 1.0 C/1.0 C at 60 °C.

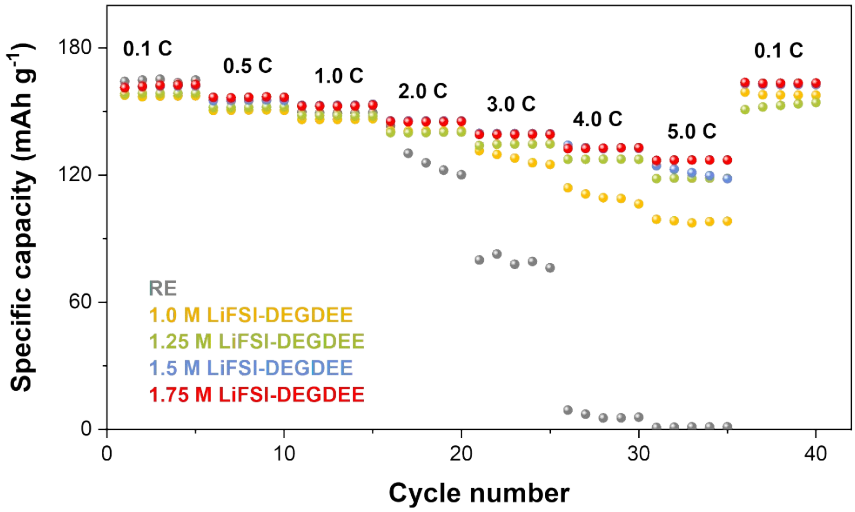

Fig. S14. Rate performance of Li||LFP cells with different electrolytes.

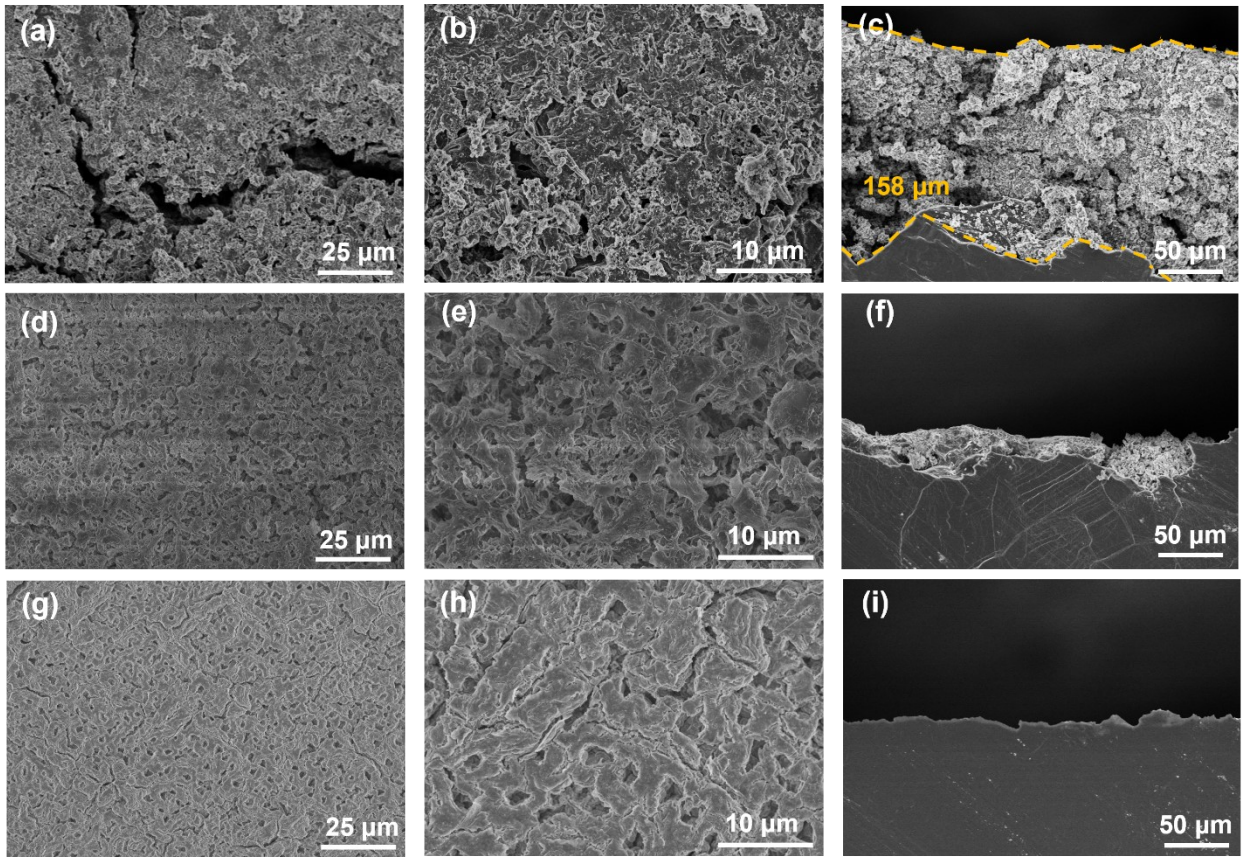

Fig. S15. The top view and cross section of Li side after cycling in Li||LFP at 0.5 C for 30 cycles in (a–c) RE, (d–f) 1.0 M LiFSI–DEGDEE, and (g–i) 1.75 M LiFSI–DEGDEE electrolytes.

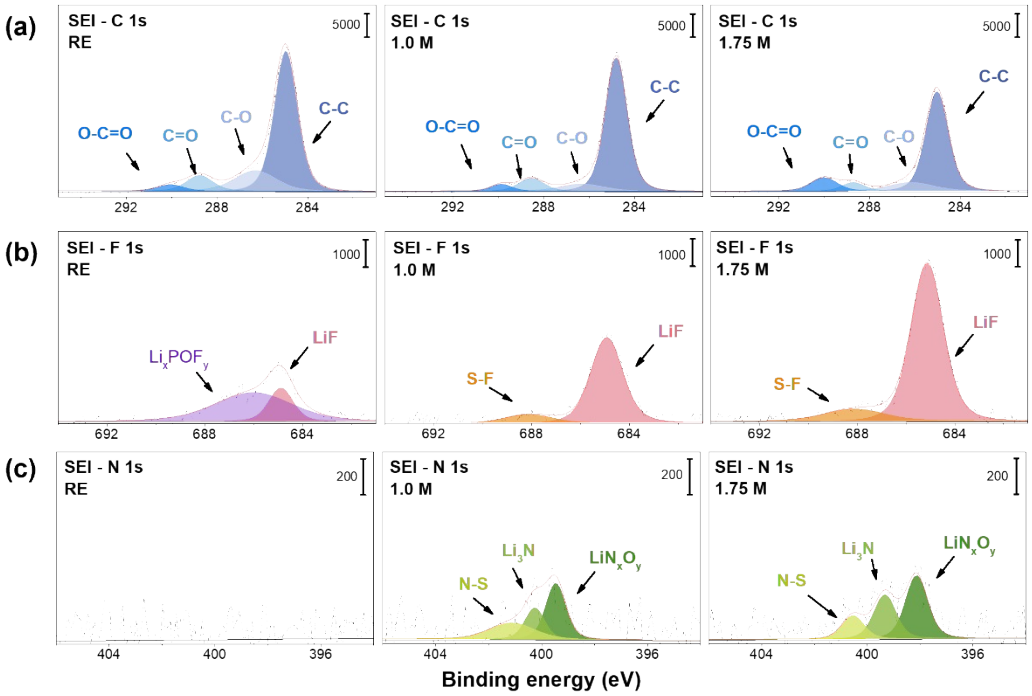

Fig. S16. XPS results for the SEI layer components on the cycled Li anodes harvested from Li||LFP at 0.5 C for 30 cycles. (a) C 1s, (b) F 1s, and (c) N 1s spectra of RE, 1.0 M and 1.75 M LiFSI in DEGDEE electrolytes.

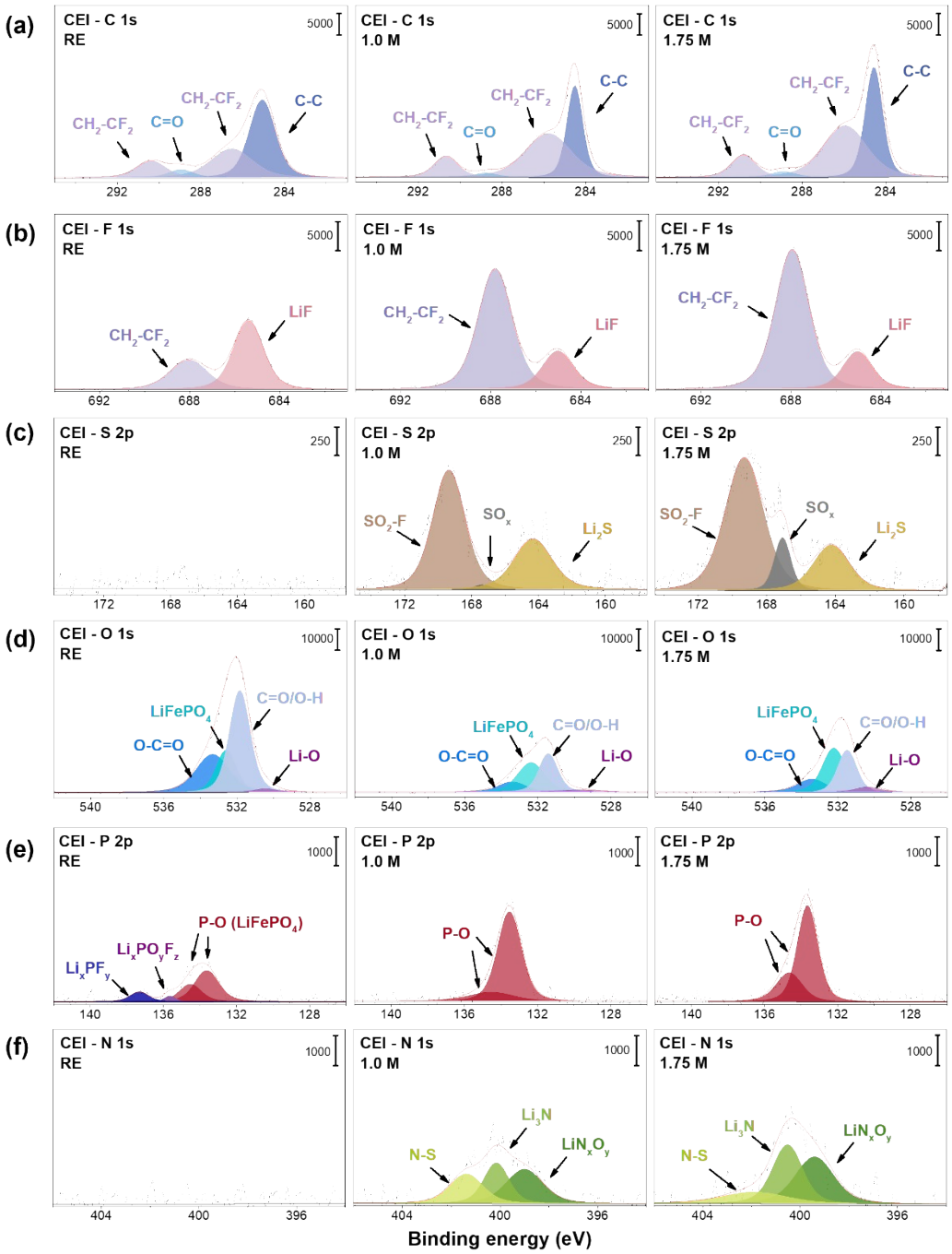

Fig. S17. XPS results for the CEI layer components on the cycled LFP cathode harvested from Li||LFP at 0.5 C for 30 cycles. (a) C 1s, (b) F 1s, (c) S 2p, (d) O 1s, (e) P 2p, and (f) N 1s spectra of RE, 1.0 M and 1.75 M LiFSI in DEGDEE electrolytes.

Table S1. Physical properties of different common carbonate and linear ether solvents.

Properties	DME	DEE	DEGDME	DEGDEE	EC	EMC	DMC
Density (g ml^{-1})	0.86	0.84	0.95	0.91	1.32	1.01	1.07
Melting point (°C)	−69.2[a]	−74[a]	−68[b]	−44[b]	36.4[a]	-55[a]	4[a]
Boiling point (°C)	85[a]	121.2[a]	162[b]	188[b]	248[a]	110[a]	90[a]
Flash point (°C)	−6[a]	27-35 [a]	51-57[b]	70[b]	160[a]	23[a]	0.76[a]
Vapor pressure (mm Hg)	54[a]	9.4[a]	2-3[b]	0.5[1]	0[a]	27[a]	18[a]
Donor number (kcal mol^{-1})	20 [2,3]	19.2[2]	18[3]	-	16.4[4]	6.5[4]	8.7[4]
Dielectric constant	7.3[5]	3.9[5]	7.3[6]	5.7[6]	90 (40 °C)[5]	2.9[5]	3.1[5]
Dipole moment (D)	1.71[2]	1.65[2]	1.92[6]	1.96[6]	4.61[7]	0.89[7]	0.76[7]
Viscosity (cP)	0.46[2]	0.73	0.98	1.12	1.9 (40 °C)[4,7]	0.65[4,7]	0.59[4,7]
Surface tension (mN m^{-1})	23.9[8]	-	24.8[9]	26 (20 °C)[10]	-	-	28.5[9,11,12]

DME: 1,2-dimethoxyethane, DEE: 1,2-diethoxyethane, DEGDME: diethylene glycol dimethyl ether, DEGDEE: diethylene glycol diethyl ether, EC: ethylene carbonate, EMC: ethyl methyl carbonate, DMC: dimethyl carbonate.

**Note:* Values are sourced from (a) Sigma-Aldrich and (b) TCI. Viscosity was measured in this work at 25°C.

Table S2. Comparison of our work with state-of-the-art electrolytes at 25°C.

No.	Electrolyte	Ionic conductivity (mS cm^{-1})	Viscosity (cP)	Current density (mA cm^{-2})	Areal capacity (mAh cm^{-2})	CE (Li||Cu)	Capacity retention (Li||LFP)	Ref.
1	1.75 M LiFSI-DEGDEE	5.06	12.1	1.0	1.0	~98 % (300 cycles)	~80 % (1000 cycles)	**This work**
2	1.0 M LiFSI-DEGDEE	5.16	4.06	1.0	1.0	~98 % (120 cycles)	~80 % (400 cycles)	**This work**
3	1.0 M LiFSI-DME	16.8	1.51	0.5	0.5	~90 % (100 cycles) Fluctuation	~72.3 % (200 cycles)	[13]
4	1.0 M LiFSI-DEE	7.8	2.21	0.5	0.5	~98 % (100 cycles)	~93.5 % (200 cycles)	[13]
5	1.0 M LiFSI-DEGDME	7.6	10.1	0.5	1.0	~70 % (100 cycles) Fluctuation	None	[14]
6	3.57 M LiTFSI–DME	2.01	64.84	0.5	1.0	~95 % (175 cycles) Fluctuation	~92 % (100 cycles)	[15]
7	4.2 M LiDFP–DME	0.45	8.02	0.5	1.0	~91 % (200 cycles) Fluctuation	~57 % (100 cycles)	[15]
8	4.0 M LiODFB-DME	1.99	118	1.0	1.5	~90 % (50 cycles) Unstable	~99 % (200 cycles) Fluctuation	[16]
9	1.0 M $LiPF_6$-EC:EMC:DMC (1:1:1, vol.)	10.48	3.187	-	-	None	None	[17]

Table S3. Transference number of Li^+ (t_+) in DEGDEE-based electrolytes.

Electrolyte	t_+
1.0 M LiFSI-DEGDEE	0.43 ± 0.02
1.25 M LiFSI-DEGDEE	0.43 ± 0.01
1.5 M LiFSI-DEGDEE	0.44 ± 0.01
1.75 M LiFSI-DEGDEE	0.45 ± 0.00

Table S4. Electrochemical stability windows (ESW) of the electrolytes measured using LSV.

Concentration (M)	Reduction potential (V *vs.* Li/Li^+)	Oxidation potential (V *vs.* Li/Li^+)	ESW (V *vs.* Li/Li^+)
1.75	-0.12	4.88	5.0
1.5	-0.09	4.89	4.99
1.25	-0.07	4.90	4.97
1.0	-0.04	4.90	4.94

Table S5. XPS binding energy (eV) corresponding to the deconvoluted peaks for the surface of Cu substrates with Li deposited.

	Components	Binding energy (eV)			Ratio of components (%)			Reference
		RE	1.0 M	1.75 M	RE	1.0 M	1.75 M	
C 1s	C-C	285.29	284.97	284.91	68.50	81.01	55.61	[15,18]
	C-O	286.42	286.53	286.12	18.04	6.47	23.03	[15,19]
	C=O	289.07	288.72	288.64	5.34	9.29	4.61	[19]
	O-C=O	289.99	289.98	289.93	3.97	3.24	16.75	[15]
	Li_2CO_3	290.70	-	-	4.15	-	-	[19,20]
F 1s	LiF	685.10	685.02	685.15	83.95	92.07	96.04	[15,19,21]
	S-F	-	687.84	687.95	-	7.93	3.96	[15,21]
	Li_xPOF_y	688.56	-	-	16.08	-	-	[22]

Table S6. XPS binding energy (eV) corresponding to the deconvoluted peaks for the surface of Li electrodes.

	Components	Binding energy (eV)			Reference
		RE	1.0 M	1.75 M	
C 1s	C-C	284.94	284.78	284.98	[15,18]
	C-O	286.28	286.27	286.24	[15,19]
	C=O	288.75	288.52	288.68	[19]
	O-C=O	290.03	289.85	289.97	[15]
F 1s	LiF	685.18	685.19	685.10	[19,20]
	Li_xPOF_y	686.27	-	-	[15,19,21]
	S-F	-	688.09	688.08	[15,21]
N 1s	LiN_xO_y	-	398.94	398.90	[20]
	Li_3N	-	399.99	399.90	[20]
	N-S	-	401.10	400.95	[20]

Table S7. XPS binding energy (eV) corresponding to the deconvoluted peaks for the surface of LFP electrodes.

Components		Binding energy (eV)			Reference
		RE	1.0 M	1.75 M	
C 1s	C-C	285.05	284.50	284.53	[15]
	C=O	288.93	288.76	288.87	[15]
	CH_2-CF_2	286.50	285.81	285.92	[23]
		290.37	290.65	290.78	[23]
F 1s	LiF	685.37	685.00	685.01	[15]
	CF_2-CF_2	688.03	687.78	687.92	[2]
S 2p	Li_2S	-	164.30	164.09	[18,20,21]
	SO_x	-	167.34	167.16	[18,20]
	SO_2-F	-	169.34	169.27	[18,20,21]
O 2p	Li-O	530.42	530.73	530.88	[15]
	C=O/O-H	531.82	531.41	531.54	[15]
	$LiFePO_4$	532.57	532.35	532.19	[2]
	O-C=O	533.31	533.38	533.28	[15]
P 2p	P-O	133.61	133.56	133.61	[15,22,24]
		134.50	134.50	134.61	[15,22,24]
	Li_xPOF_y	135.64	-	-	[22,24]
	Li_xPF_y	137.30	-	-	[24]
N 1s	LiN_xO_y	-	398.98	399.38	[20]
	Li_3N	-	400.13	400.49	[20]
	N-S	-	401.36	401.86	[20]

Reference

1 S. Tang and H. Zhao, *RSC Adv*, 2014, **4**, 11251–11287.

2 T. D. Pham, K.-K. Lee, T. D. K. Pham and -K Lee, *Small*, 2021, **17**, 2100133.

3 R. J. Gomes, C. Birch, M. M. Cencer, C. Li, S. B. Son, I. D. Bloom, R. S. Assary and C. V. Amanchukwu, *Journal of Physical Chemistry C*, 2022, **126**, 13595–13606.

4 D. Zhu, Y. Ren, Y. Yu, L. Zhang, Y. Wan, H. Wang, W. Gao, B. Han and L. Zhang, *ChemElectroChem*, DOI:10.1002/CELC.202300009.

5 *CRC Handbook of Chemistry and Physics*, DOI:10.1201/9781315380476.

6 R. Stenutz, Tables for Organic Chemistry, https://www.stenutz.eu/chem/, (accessed 9 May 2025).

7 K. Xu, *Chem Rev*, 2004, **104**, 4303–4417.

8 G. Zhao, S. Bi, X. Li and J. Wu, *Fluid Phase Equilib*, 2010, **295**, 46–49.

9 S. Osman, O. Nuri Şara, A. Altun Kavaklı, M.-J. Lungu and S. Osman, *Journal of Thermal Analysis and Calorimetry 2024 149:23*, 2024, **149**, 14489–14513.

10 X. X. Li, Y. X. Liu and X. H. Wei, *J Chem Eng Data*, 2004, **49**, 1043–1045.

11 F. Wang, J. Wu and Z. Liu, *Fluid Phase Equilib*, 2004, **220**, 123–126.

12 J. J. Jasper, *J Phys Chem Ref Data*, 1972, **1**, 841–1010.

13 T. D. Pham, A. Bin Faheem, J. Kim, H. M. Oh, K.-K. Lee, T. D. Pham, A. Bin Faheem, J. Kim, K.-K. Lee and H. M. Oh, *Small*, 2022, **18**, 2107492.

14 J. You, Q. Wang, R. Wei, L. Deng, Y. Hu, L. Niu, J. Wang, X. Zheng, J. Li, Y. Zhou and J. T. Li, *Nanomicro Lett*, 2024, **16**, 1–19.

15 T. Duong Pham, A. Bin Faheem, S. Yeon Chun, J.-R. Rho, K. Kwak, K.-K. Lee, T. D. Pham, A. Bin Faheem, K. Lee, S. Y. Chun, K. Kwak and J. Rho, *Adv Energy Mater*, 2021, **11**, 2003520.

16 S. Jiao, X. Ren, R. Cao, M. H. Engelhard, Y. Liu, D. Hu, D. Mei, J. Zheng, W. Zhao, Q. Li, N. Liu, B. D. Adams, C. Ma, J. Liu, J. G. Zhang and W. Xu, *Nat Energy*, 2018, **3**, 739–746.

17 W. Liu, J. Li, W. Li, H. Xu, C. Zhang and X. Qiu, *Nature Communications 2020 11:1*, 2020, **11**, 1–11.

18 K. Lee, S. H. Kwon, J. Kim, E. Park, I. Kim, H. C. Ahn, A. Coskun and J. W. Choi, *ACS Energy Lett*, 2024, **9**, 2201–2211.

19 B. Yang, H. Zhang, L. Yu, W. Z. Fan and D. Huang, *Electrochim Acta*, 2016, **221**, 107–114.

20 Z. Wang, C. Chen, D. Wang, Y. Zhu and B. Zhang, *Angewandte Chemie International Edition*, DOI:10.1002/anie.202303950.

21 R. Miao, J. Yang, Z. Xu, J. Wang, Y. Nuli and L. Sun, *Scientific Reports 2016 6:1*, 2016, **6**, 1–9.

22 P. Shi, L. Zhang, H. Xiang, X. Liang, Y. Sun and W. Xu, *ACS Appl Mater Interfaces*, 2018, **10**, 22201–22209.

23 T. D. Pham, A. Bin Faheem, H. D. Nguyen, H. M. Oh and K. K. Lee, *J Mater Chem A Mater*, 2022, **10**, 12035–12046.

24 H. Lee, H. S. Lim, X. Ren, L. Yu, M. H. Engelhard, K. S. Han, J. Lee, H. T. Kim, J. Xiao, J. Liu, W. Xu and J. G. Zhang, *ACS Energy Lett*, 2018, **3**, 2921–2930.